ACS OMEGA

Open Access

http://pubs.acs.org/journal/acsodf

Article

Platinum Nanoparticles Bonded with Carbon Nanotubes for High-Performance Ampere-Level All-Water Splitting

Hong Tang, Takahiro Kojima, Kenji Kazumi, Kazuhiro Fukami, and Hiroshi Sakaguchi*

Cite This: *ACS Omega* 2024, 9, 21378−21387

Read Online

ACCESS | Metrics & More | Article Recommendations | Supporting Information

ABSTRACT: Platinum nanoparticles loaded on a nitrogen-doped carbon nanotubes exhibit a brilliant hydrogen evolution reaction (HER) in an alkaline solution, but their bifunctional hydrogen and oxygen evolution reaction (OER) has not been reported due to the lack of a strong Pt−C bond. In this work, platinum nanoparticles bonded in carbon nanotubes (Pt-NPs-bonded@CNT) with strong Pt−C bonds are designed toward ultralow overpotential water splitting ability in alkaline solution. Benefit from the strong interaction between platinum and high conductivity carbon nanotube substrates through the Pt−C bond also the platinum nanoparticles bonded in carbon nanotube can provide more stable active sites, as a result, the Pt-NPs-bonded@CNT exhibits excellent hydrogen evolution in acid and alkaline solution with ultralow overpotential of 0.19 and 0.23 V to reach 1000 mA cm^{-2}, respectively. Besides, it shows superior oxygen evolution electrocatalysis in alkaline solution with a low overpotential of 1.69 V at 1000 mA cm^{-2}. Furthermore, it also exhibits high stability over 110 h against the evolution of oxygen and hydrogen at 1000 mA cm^{-2}. This strategy paves the way to the high performance of bifunctional electrocatalytic reaction with extraordinary stability originating from optimized electron density of metal active sites due to strong metal-substrate interaction.

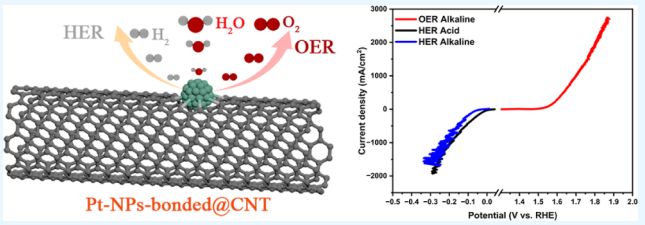

1. INTRODUCTION

Hydrogen fuel has become the most important fuel in the world today, besides fossil fuels, due to its high energy density and product cleanliness.[1−3] However, a large amount of energy is consumed in the process of industrial hydrogen production as the result of the constant need for high overpotential for water splitting, especially in an alkaline medium, and the low proton concentration has become a serious obstacle for HER.[4,5] In fact, developing water electrolysis catalysts for industrial applications is very challenging because they always face the bottleneck of long-term stability and low overpotential when operating at ampere-level current. The anion exchange membrane (AEM) based water electrolyzer also relies on an efficient oxygen evolution reaction (OER), so the application of highly active catalysts to evolve oxygen under alkaline conditions has become a thorny issue.[6−8] Platinum is a milestone catalyst that has achieved hydrogen evolution under acidic conditions, but it is also hindered by the magnitude of low reaction kinetics in alkaline solution compared with acidic medium due to the key water dissociation step ($H_2O + e^- \rightarrow *H + OH^-$).[9,10]

Given the hydrogen evolution capability under acidic conditions, developing Pt-based electrocatalysts with low cost, fast kinetics, and long-term stability in alkaline solutions has become an important strategy worth exploring. In previous studies, many efforts have been devoted to designing Pt-based catalysts to enhance their hydrogen evolution ability.[11−13] A common understanding for devising the strategy is that the improvement of catalytic performance mainly includes two key aspects: (1) Increase the specific surface area of the catalyst to expose more active sites, such as nanoparticles, nanoclusters, nanoplates, and metal−organic frameworks, thereby making the electrode have more active sites to combine intermediates for improving the catalytic performance.[14−18] (2) Construct Pt-based composite materials by confining active sites into other electrochemically active materials or converting platinum metal to platinum compounds, such as oxide, telluride, and alloys.[19−22]

The splendid oxygen evolution performance of platinum-based materials has rarely been studied, and achieving platinum-based catalysts with efficient bifunctional hydrogen and oxygen evolution ability is an important research field because the oxygen evolution reaction is also a pivotal part of the anion exchange membrane water electrolyzer.[23] In order to construct an efficient platinum-based catalyst for water splitting, choosing a suitable substrate to load active platinum with a stable structure to serve strong metal−support interaction is an important point.[24−27] Carbon nanotube

Received: February 20, 2024
Revised: April 17, 2024
Accepted: April 25, 2024
Published: April 30, 2024

(CNT), as a stable high conductivity substrate, is most promising for anchoring active sites on the surface toward high-activity catalysts, such as nanoparticles, nanoplates, and nanowires.[16,28−30] Wang et al. reported that successfully synthesized Pt nanoparticles loaded on nitrogen-doped carbon nanotubes with pyridinic-N and pyrrolic-N decorated, have shown ampere-level hydrogen evolution ability, but did not exhibit OER performance due to the lack of strong Pt−C bonds.[31] Meanwhile, previous research is limited to achieving significant bifunctional hydrogen and oxygen evolution based on platinum and CNT through strong chemical bond interaction to reduce electron transfer energy barriers.

Inspired by the above discussion, herein, we designed platinum nanoparticles bonded in carbon nanotubes (Pt-NPs-bonded@CNT) with Pt−C bonds toward ultralow overpotential water splitting ability in alkaline solution (Figure 1).

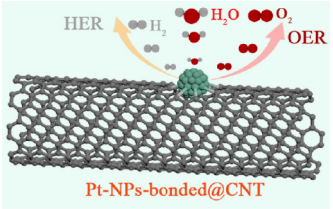

Figure 1. Schematic illustration of Pt-NPs-bonded@CNT toward bifunctional catalytic hydrogen evolution reaction (HER) and oxygen evolution reaction (OER).

During the synthesis process, carbon nanotubes are employed as the substrate, and surface oxygen-containing groups of carbon nanotubes are modified by strong acid treatment, causing defects on the surface to capture platinum atoms, thereby promoting the embedding of platinum nanoparticles on the surface of carbon nanotubes. Benefit from the strong interaction between platinum and high-conductivity carbon nanotube substrates through the Pt−C bond, the platinum nanoparticles bonded in carbon nanotube can provide more stable active sites, the Pt-NPs-bonded@CNT shows splendid electrocatalytic performance. Therefore, it exhibits excellent hydrogen evolution ability, and when the current density reaches 1000 mA cm^{-2}, it only requires an ultralow overpotential of 0.19 V in an acidic solution and 0.23 V in an alkaline solution. Besides, it shows superior oxygen evolution electrocatalysis in alkaline solution with a low overpotential of 1.69 V at 1000 mA cm^{-2}. Besides, it also exhibits high stability over 120 h against hydrogen evolution at 1000 mA cm^{-2} in both acid and alkaline conditions as well as long-term stability for 110 h against oxygen evolution in alkaline solution. In contrast, platinum nanoparticles attached on the surface of carbon nanotubes (Pt-NPs-attached@CNT) without Pt−C bonds are also established without acid treatment and show inferior performance for HER and no bifunctional OER performance.

2. EXPERIMENTAL SECTION

2.1. Materials Preparation. *2.1.1. Preparation of Pt-NPs-Embedded@CNT. 2.1.1.1. Acid-treated carbon nanotubes.* First, 200 mg of carbon nanotubes was hydrothermally treated in 30 mL of 5 M nitric acid at 160 °C for 6 h. After that, the acid-treated carbon nanotubes were collected by filtration and washed four times with deionized water to remove residual nitric acid. Then, the acid-treated carbon nanotubes were vacuum-dried for 12 h for further use.

2.1.2. Prepared Pt-NPs-Bonded@CNT. Platinum loading on acid-treated carbon nanotubes occurs through a wet chemical reaction. $H_2PtCl_6{\bullet}6H_2O$ (0.02 mmol, 10.358 mg) and acid-treated carbon nanotubes (40 mg) were dispersed in 40 mL deionized water and then kept at 90 °C for 24 h with stirring. After that, the dispersion solution was at 90 °C for 12 h to evaporate water to get the precursor powder of Pt-NPs-bonded@CNT. The obtained precursor of Pt-NPs-bonded@CNT was annealed at 900 °C for 2 h under an argon atmosphere and cooling naturally.

2.1.3. Prepared the Pt-NPs-Attached@CNT. The Pt-NPs-attached@CNT was prepared by the same procedure except that the carbon nanotubes were not treated with acid.

2.2. Electrochemical Measurement. Electrochemical performance tests of all catalysts were performed on an electrochemical workstation using a three-electrode system. The electrolyte used in all tests under alkaline and acidic conditions was 1.0 M KOH and 0.5 M H_2SO_4 solution, respectively. When testing the hydrogen evolution reaction, a graphite electrode was used as the counter electrode, besides, an Ag/AgCl electrode and Hg/HgO electrode were used as reference electrodes in acid and alkaline solutions, respectively. When testing the oxygen evolution reaction under alkaline conditions, a platinum plate electrode was used as the counter electrode. The Pt-NPs-bonded@CNT electrode was obtained by drop-dry mothed. Briefly, 5 mg of Pt-NPs-bonded@CNT catalyst was first dispersed in a mixed solution of 50 μL of Nafion dispersion, 450 μL isopropyl alcohol and 500 μL water. Afterward, drop 40 μL of Pt-NPs-bonded@CNT dispersion evenly on the surface of the carbon paper electrode, and then use it to test the electrochemical performance after natural drying for 2 h. The Pt−C electrode was prepared using the same method. Polarization curves were measured by linear sweep voltammetry (LSV) at a sweep rate of 5 mV s^{-1}. All obtained LSV curves were corrected with 100% *iR* compensation. All stability measurements were performed using potentiostat testing at 1000 mA cm^{-2} for over 100 h. Electrochemical impedance spectroscopy (EIS) was tested in the frequency range from 10000 to 0.1 Hz with an amplitude voltage of 5 mV.

The conversion of the test potential into a potential relative to a reversible hydrogen electrode (RHE) under acidic conditions can be calculated by using the Nernst equation:

$$E_{RHE} = E_{Ag/AgCl} + 0.198 + 0.0591 \times pH$$

Under alkaline conditions, due to changes in the reference electrode, the Nernst equation that converts the potential of the reversible hydrogen electrode is:

$$E_{RHE} = E_{Hg/HgO} + 0.098 + 0.0591 \times pH$$

The Tafel slope (b) is obtained by linear fitting a plot derived from the logarithm of current density (j) versus overpotential (η) through follow equation:

The electrochemical double layer capacitance (C_{dl}) is obtained by cyclic voltammetry (CV) measurement at various scan rates with a voltage of −0.7∼−0.9 V versus $E_{Hg/HgO}$.

3. RESULTS AND DISCUSSION

3.1. Phase and Structural Characterizations. Pt-NPs-bonded@CNT with platinum nanoparticles bonded in carbon

https://doi.org/10.1021/acsomega.4c01662
ACS Omega 2024, 9, 21378−21387

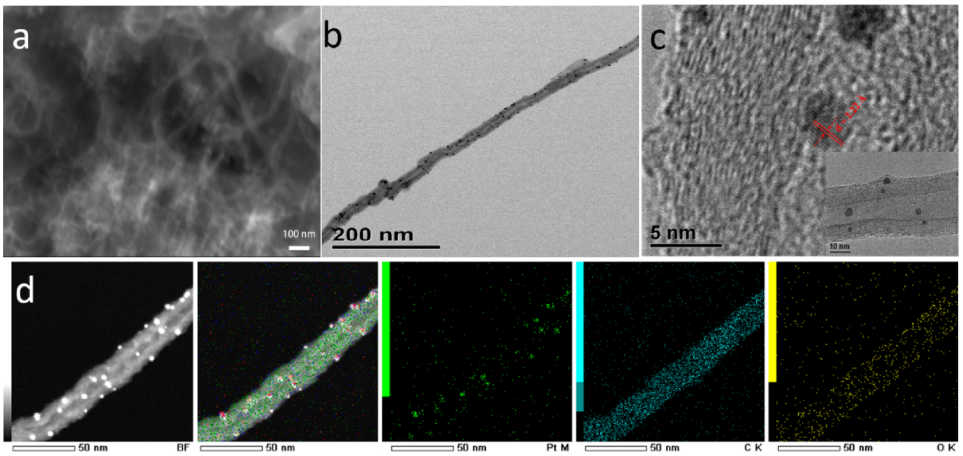

Figure 2. (a) SEM image of the Pt-NPs-bonded@CNT. (b, c) TEM and HR-TEM of Pt-NPs-bonded@CNT. (d) EDS mapping of Pt-NPs-bonded@CNT.

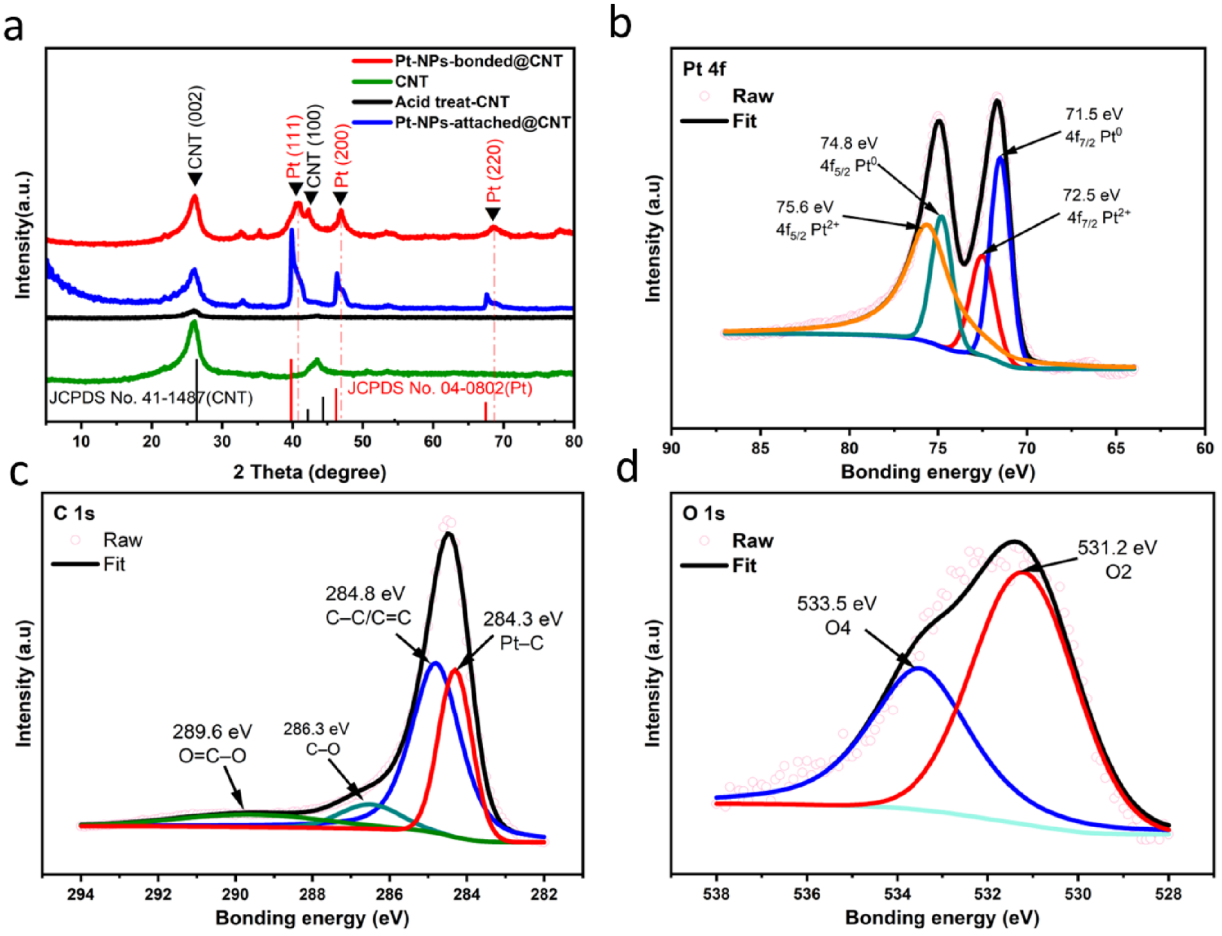

Figure 3. (a) XRD patterns of Pt-NPs-bonded@CNT (red), Pt-NPs-attached@CNTs (blue), acid- treated CNTs (black), and CNT (green). The XRD standard card data for Pt (JCPDS No. 04−0802) and CNT (JCPDS No. 41−1487) are marked in red and black. (b−d) Pt 4f, C 1s, and O 1s high resolution of XPS spectra of Pt-NPs-bonded@CNT.

nanotubes was prepared through in situ-growth of platinum nanoparticles on the surface of carbon nanotubes with defects, as illustrated in Figure S1. First, defects, which means holes, oxidative functional groups, such as hydroxyl and carboxyl groups, were formed on carbon nanotubes surface after hydrothermal acidification treatment. After that, the defective carbon nanotubes and platinum source were dispersed in deionized water, the platinum ions captured by the defect sites during medium temperature and then evaporation water to get precursor of Pt-NPs-bonded@CNT. Finally,Pt-NPs-bonded@CNT precursor was annealed at high temperature to get the final product. Scanning electron microscopy (SEM) and transmission electron microscopy (TEM) measurements are carried out to authenticate the morphological information on

https://doi.org/10.1021/acsomega.4c01662
ACS Omega 2024, 9, 21378−21387

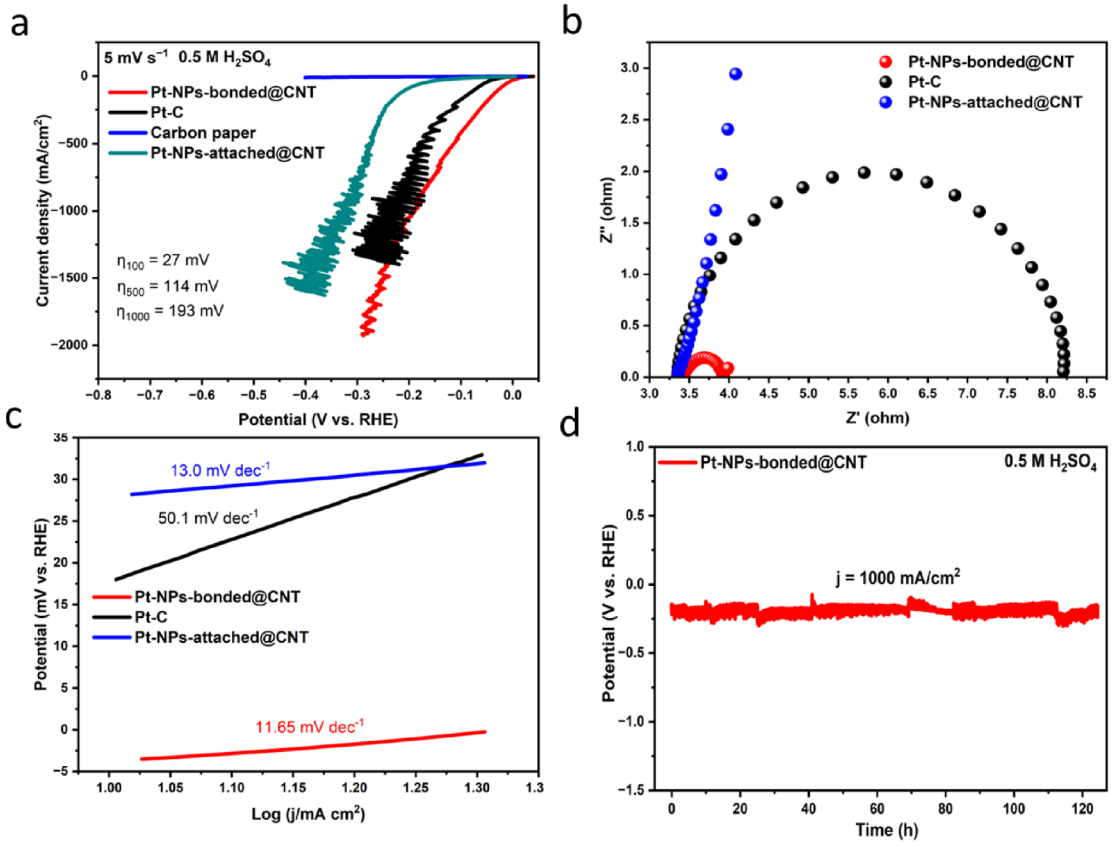

Figure 4. HER electrochemical performance measurements in acid. (a) HER LSV curves of Pt-NPs-bonded@CNT, Pt−C, and Pt-NPs-attached@CNT, and carbon paper in 0.5 M H_2SO_4. (b) EIS of Pt-NPs-bonded@CNT, Pt−C, and Pt-NPs-attached@CNT in 0.5 M H_2SO_4. (c) Tafel slope comparison graph of Pt-NPs-bonded@CNT, Pt−C, and Pt-NPs-attached@CNT. (d) Galvanostatic hydrogen evolution measurement of the Pt-NPs-bonded@CNT at 1000 mA cm^{-2} in 0.5 M H_2SO_4.

the Pt-NPs-bonded@CNT. As shown in Figure 2a, the SEM image shows a smooth carbon nanotube shape after loading platinum particles on the acid-treated carbon nanotube surface. TEM and HAADF-STEM images demonstrated that the platinum nanoparticles are bonded on the surface of the carbon nanotube and are only a few nanometers in diameter, which is beneficial to expose more active sites for absorbed intermediates to enhance electrocatalytic performance (Figures 2b and S4). Furthermore, the HR-TEM image more clearly displays the platinum nanoparticles bonded on the surface of the carbon nanotube and covered by an amorphous carbon nanolayer (inset of Figure 2c). Figure 2c reveals that the platinum nanoparticles have a single interplanar spacing of 2.22 Å of the Pt (111) facet, which is the slightly shrunken typical interplanar spacing of 2.27 Å of the standard Pt (111) crystal face.[32] This result is also consistent with the Fourier transform of the platinum lattice and the selective electron area diffraction (SAED) pattern (Figures S5 and S6). Moreover, energy-dispersive X-ray spectroscopy (EDS) elemental mapping confirmed that the bright spots on the carbon nanotubes were platinum nanoparticles (Figure 2d). The mass loading of Pt nanoparticles in the nanocomposites is 0.7 wt %, which is within the appropriate value range for high catalytic performance in the relevant literature.[33] Additionally, the C and the O elements are uniformly distributed in the Pt-NPs-bonded@CNT, and the O elements have very little content. In contrast, the TEM image of Pt-NPs-attached@CNT shows that platinum nanoparticles are supposed to be only attached on the surface of carbon nanotubes, and the platinum nanoparticles exhibit an amorphous structure (Figure S7). The elemental mapping image also verified the distribution information on platinum nanoparticles as well as the C and O elements in Pt-NPs-attached@CNTs.

The crystal structure of Pt-NPs-bonded@CNT is revealed by X-ray diffraction (XRD) pattern, as present in Figure 3a. These diffraction peaks can be well matched with metal platinum (JCPDS No. 04−0802 (Pt)), and no impurity peak, such as platinum oxide, appears, indicating the formation of high pure phases of platinum nanoparticles. Nevertheless, all peaks of platinum are upshifted compared to the standard of platinum. This result is caused by a slight shrinkage in the interplanar spacing of the platinum nanoparticle lattice, which is consistent with the HR-TEM result of the slightly shrunk Pt (111) facet and the Bragg equation of the XRD calculation results (0.05 Å). Besides, the diffraction peak position (JCPDS No. 41−1487 (CNT)) of the XRD pattern of the carbon nanotube after acid treatment is not changed compared to the pristine carbon nanotube, however, the intensity of the diffraction peak becomes weaker, which is due to defects created on the surface of the carbon nanotube.[34] It is worth noting that the peak of Pt-NPs-bonded@CNT at 42.2° belongs to the (100) peak of CNT because it matches well with the (100) peak of JCPDS No. 41−1487 (CNT) (Figure 3a). Besides, there is no shift in the position of the platinum peak of Pt-NPs-attached@CNTs, which further confirms that the platinum nanoparticles are attached to the surface of CNTs without any stress, causing slight deformation of the platinum crystal lattice. As a result, we conclude that the pure platinum

https://doi.org/10.1021/acsomega.4c01662
ACS Omega 2024, 9, 21378−21387

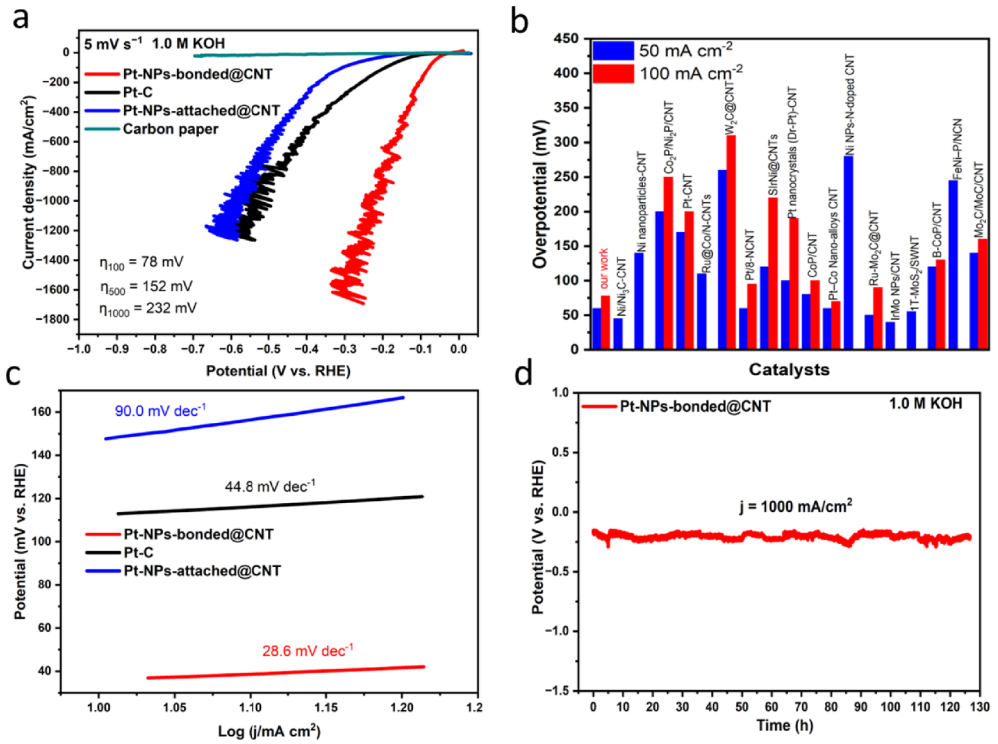

Figure 5. HER electrochemical performance measurements in alkaline. (a) HER LSV curves of Pt-NPs-bonded@CNT, Pt-NPs-attached@CNT, Pt−C, and carbon paper in 1.0 M KOH. (b) Comparison of the overpotential graph of Pt-NPs-bonded@CNT with excellent CNT-based materials at 50 mA cm^{-2} and 100 mA cm^{-2}. (c) Tafel slope compared graph of Pt-NPs-bonded@CNT, Pt−C, and Pt-NPs-attached@CNT. (d) Galvanostatic hydrogen evolution measurement of the Pt-NPs-bonded@CNT at 1000 mA cm^{-2} in 1.0 M KOH.

nanoparticles bonded on the surface of the carbon nanotube and the presence of platinum oxides is ruled out.

The chemical state of the surface elements of Pt-NPs-bonded@CNTs was determined by X-ray photoelectron spectroscopy (XPS), as shown in Figure 3b−d. The chemical valence of platinum is detected by the spectrum of Pt 4f, as displayed in Figure 3b. There are two peaks located at 75.6 and 72.5 eV, which are attributed to the $4f_{5/2}$ orbital of Pt^{2+} and $4f_{7/2}$ orbital of Pt^{2+}, respectively.[31] Meanwhile, the peaks that appeared at 74.8 and 71.5 eV are ascribed to Pt metallic states. Four peaks appeared at 284.3 eV, 284.8 eV, 286.3 eV, and 289.6 eV in the high-resolution XPS spectrum of C 1s, which is attributed to Pt−C, C−C/C=C, C−O, and O=C−O bonds in carbon nanotubes, respectively (Figure 3c).[35,36] The existence of C−O and O=C−O bonds found in carbon nanotubes verified that the surface modification is successful and oxygen-containing groups are formed on the surface of carbon nanotubes. Besides, the spectrum of the O 1s is also used to check the platinum chemical state indirectly. There are only O2 and O4 peaks located at 531.2 and 533.5 eV, which are related to hydroxyl groups and adsorbed water (Figure 3d).[37] However, the O1 peak associated with metal oxides and the O3 peak belonging to lattice-defective oxygen on the metal surface are all absent, which can illustrate there are no platinum oxides existing in Pt-NPs-bonded@CNT.[38] This result demonstrates that divalent platinum is formed by the formation of chemical bonds between platinum and carbon (Pt−C) in carbon nanotubes. The metallic state of platinum is related to the platinum nanoparticles bonded in carbon nanotubes. In contrast, for Pt-NPs-attached@CNTs, the chemical valence of platinum shown in the Pt 4f spectrum is almost that of the Pt metallic state due to the lack of Pt−C bond and only a very weak peak of divalent platinum because the O 1s spectrum shows the presence of oxygen defects in platinum nanoparticles. In addition, the Pt−C peak at 284.3 eV in the C 1s spectrum also disappeared, which confirms that the connection between platinum nanoparticles and CNTs lacks Pt−C bonds (Figure S9).

3.2. Electrocatalysis Performance of HER in 0.5 M H_2SO_4. The hydrogen evolution ability of the Pt-NPs-bonded@CNT electrode under acidic conditions was systematically tested, as shown by the linear sweep voltammetry (LSV) curves in Figure 4a. Compared to Pt−C, Pt-NPs-attached@CNT, and carbon paper, the Pt-NPs-bonded@CNT electrode exhibits the best HER performance and reaches ampere-level current density with a small overpotential. It is worth noting that the Pt-NPs-bonded@CNT electrode only requires an overpotential of 27 and 114 mV to reach 100 mA cm^{-2} and 500 mA cm^{-2}, and even only needs 193 mV to achieve an ampere-level current density of 1000 mA cm^{-2}, which is significantly outperforming the benchmark electrocatalyst of Pt−C with an overpotential of 73 mV (η_{100}), 181 mV (η_{500}), and 234 mV (η_{1000}). In addition, its HER performance also exceeds that of Pt-NPs-attached@CNTs without acid treatment, which is 200 mV (η_{100}), 275 mV (η_{500}), and 324 mV (η_{1000}). The substrate of carbon paper shows a negligible ability for hydrogen evolution. The resulting low overpotential of Pt-NPs-bonded@CNT is attributed to the platinum nanoparticle bonded in the carbon nanotube with Pt−C bond, resulting in an efficiently reduced electron transfer energy barrier, and highly dispersed platinum nanoparticles providing more adsorption active sites for hydrogen radicals. Electrochemical impedance spectroscopy (EIS) of Pt-NPs-bonded@CNT, Pt-NPs-attached@CNT and Pt−C reveals the

https://doi.org/10.1021/acsomega.4c01662
ACS Omega 2024, 9, 21378−21387

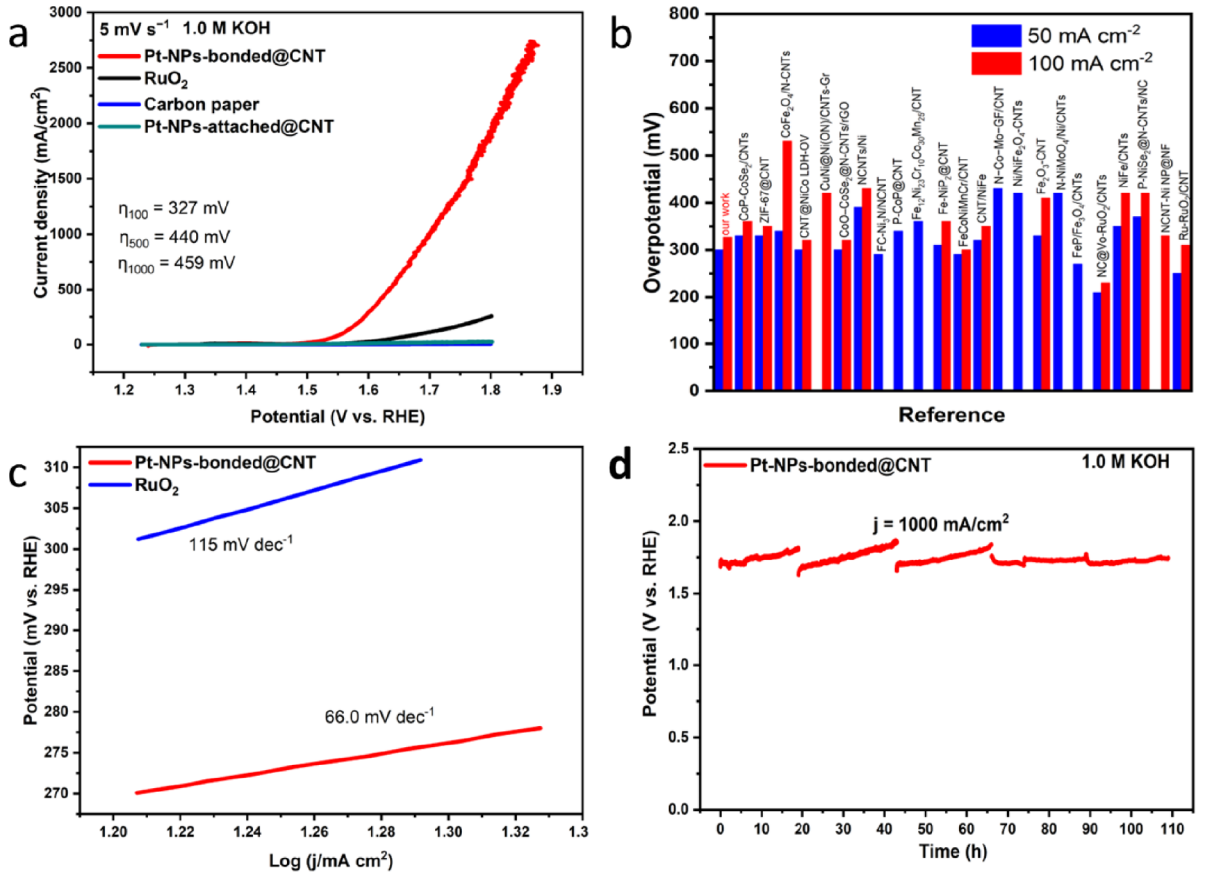

Figure 6. OER Electrochemical performance measurements in alkaline. (a) OER LSV curves of Pt-NPs-bonded@CNT, RuO_2, and Pt-NPs-attached@CNT, and carbon paper in 1.0 M KOH. (b) Comparison of the overpotential graph of Pt-NPs-bonded@CNT with excellent CNT-based materials at 50 mA cm^{-2} and 100 mA cm^{-2}. (c) Tafel slope comparison graph of Pt-NPs-bonded@CNT and RuO_2 of the OER in 1.0 M KOH. (d) Galvanostatic oxygen evolution measurement of the Pt-NPs-bonded@CNT at 1000 mA cm^{-2} in 1.0 M KOH.

electron transfer energy barrier corresponding to the charge transfer properties, as displayed in Figure 4b. In the Nyquist plots, the Nyquist semicircle diameter represents the charge transfer resistance (R_{ct}). The Pt-NPs-bonded@CNT exhibits the lowest charge transfer resistance (R_{ct}) compared with Pt-NPs-attached@CNT and Pt−C, which means that the Pt-NPs-bonded@CNT has faster electron transfer properties, thereby accelerating water splitting.[39,40] Tafel slope is usually used as an indicator of hydrogen evolution ability. In Figure 4c, the Tafel slopes are illustrated based on the corresponding LSV curves shown in Figure 4a. The Pt-NPs-bonded@CNT exhibits the smallest Tafel slope value of 11.65 mV dec^{-1}, which is much smaller than the 50.1 mV dec^{-1} of Pt−C and 13.0 mV dec^{-1} of Pt-NPs-attached@CNT. The results prove that the HER process is dominated by the Volmer−Tafel route rather than the Volmer-Heyrovsky route, which is conducive to the rapid combination of hydrogen radicals to form hydrogen gas.[41] More importantly, a galvanostatic measurement of ampere-level current density catalytic hydrogen evolution stability was applied to demonstrate that the electrode can meet the requirements for electrocatalytic hydrogen evolution even at ampere-level currents required in industry. As a result, the Pt-NPs-bonded@CNT electrode can achieve long-term stability of hydrogen evolution at 1000 mA cm^{-2} for 125 h without obvious attenuation, which proves that the platinum nanoparticles bonded in the carbon nanotube maintain excellent durability even after high current density hydrogen evolution testing (Figure 4d).

3.3. Electrocatalysis Performance of HER in 1.0 M KOH. Compared with the hydrogen evolution reaction under acidic conditions, the catalyst usually exhibits poor hydrogen evolution performance under alkaline conditions due to a lack of protons. Surprisingly, the Pt-NPs-bonded@CNT also had outstanding hydrogen evolution performance in 1.0 M KOH, as presented in Figure 5a. The Pt-NPs-bonded@CNT electrode shows an obviously brilliant HER performance compared to Pt−C and Pt-NPs-attached@CNT. The measured overpotential corresponding to 100 mA cm^{-2} is 78, 195, and 307 mV for Pt-NPs-bonded@CNT, Pt−C and Pt-NPs-attached@CNT, respectively. Even at ampere-level current density, it only requires an overpotential of 232 mV, which is significantly better than the 524 mV of Pt−C and 588 mV of Pt-NPs-attached@CNT. The superb low overpotential results obtained at various current densities are better than most previously reported literature reports of splendid CNT-based catalysts, including platinum-modified carbon nanotube catalysts (Figure 5b). The Tafel slope also shows that the Pt-NPs-bonded@CNT has a much smaller value of 28.6 mV dec^{-1} compared with 44.8 mV dec^{-1} of Pt−C and 90.0 mV dec^{-1} of Pt-NPs-attached@CNT, which corresponds to the rapid water splitting ability in alkaline solution (Figure 5c). Furthermore, an ampere-level current of 1000 mA cm^{-2} was applied to evaluate the durability of the electrode, which maintained stable operation for 128 h with negligible attenuation (Figure 5d). These results indicate that Pt-NPs-bonded@CNTs with a strong Pt−C bond achieve an excellent

https://doi.org/10.1021/acsomega.4c01662
ACS Omega 2024, 9, 21378−21387

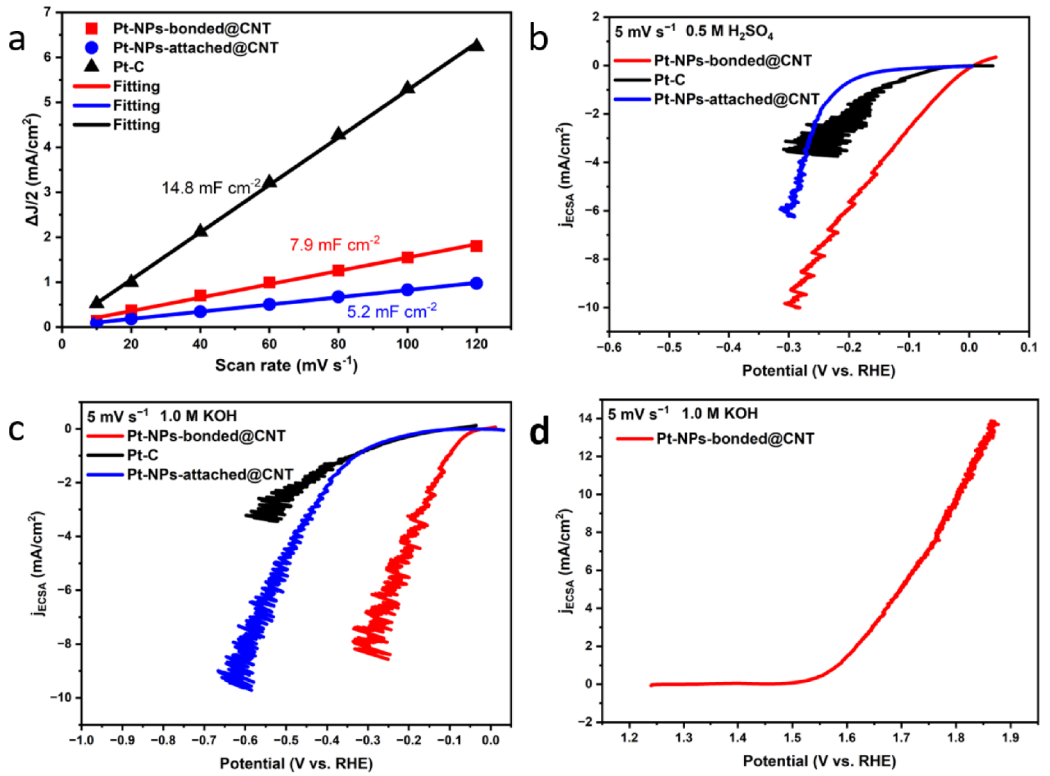

Figure 7. Electrochemical performance measurements of Pt-NPs-bonded@CNT after normalization by ECSA. (a) Relationship between current density and scan rate corresponding to cyclic voltammetry curves at different scan rates. (b) HER LSV curves normalized by ECSA in 0.5 M H_2SO_4. (c) HER LSV curves normalized by ECSA in 1.0 M KOH. (d) OER LSV curves normalized by ECSA in 1.0 M KOH.

hydrogen evolution capability even under alkaline conditions and outstanding stability even at industrial-level current densities.

3.4. Electrocatalysis Performance of OER in 1.0 M KOH. Platinum-based catalysts are rarely used for prominent oxygen evolution, even though they are a critical part of anion exchange membrane water electrolyzers. Unlike traditional platinum-based materials, which are only used for efficient hydrogen evolution, the Pt-NPs-bonded@CNT also exhibits an excellent oxygen evolution performance in alkaline solutions. As illustrated in Figure 6a, the LSV curve shows that the Pt-NPs-bonded@CNT electrode has the best oxygen evolution capability with the lowest overpotential of 1.54 and 1.69 V at 100 mA cm^{-2} and 1000 mA cm^{-2}, and its performance is significantly better than that of commercial RuO_2. The oxygen evolution capabilities of Pt-NPs-attached@CNTs and carbon paper can be ignored because the platinum nanoparticles attach on the surface of carbon paper do not exhibit strong interactions between the platinum active sites and carbon nanotube substrates. On the contrary, the excellent OER performance of Pt-NPs-bonded@CNT can be ascribed to the strong Pt−C bond regulating the activity of platinum nanoparticles through the strong interaction of metal-substrate and afford stabilizing nanoparticles bonded in carbon nanotubes. The superb low overpotential for oxygen evolution results obtained at various current densities are better than most previously reported literature of splendid CNT-based electrocatalysts (Figure 6b). Moreover, the low overpotential corresponds to the rapid water splitting ability, also according to the low Tafel slope value of 66.0 mV dec^{-1} of Pt-NPs-bonded@CNT, and the RuO_2 shows a Tafel slope value of 115 mV dec^{-1} (Figure 6c).[42,43] In order to further demonstrate the potential for practical applications, its oxygen evolution stability under an ampere-level current has also been systematically tested. There is no obvious attenuation of the overpotential after 110 h of stable operation, which also confirms that the platinum nanoparticles bonded in carbon nanotubes remain remarkably stable during oxygen evolution at ampere-scale current density (Figure 6d). Compared with Pt-NPs-bonded@CNTs, the HER/OER performance of Pt-NPs-bonded@CNTs annealed at 600 °C is poor (Figure S10).

3.5. Electrochemical Performance Measurements Normalized by ECSA. In order to identify the inherently high catalytic activity of Pt-NPs-bonded@CNT, the electrochemically active surface areas (ECSAs) of different catalysts were analyzed and estimated through a series of cyclic voltammetry (CV) tests.[44] The electrochemical active surface area affects the catalyst activity, because it reflects the active area of the catalyst participating in the reaction. It can be determined by ECSA = C_{dl}/C_s, where C_{dl} is a double-layer capacitance and C_s is the specific capacitance of the sample.[45] In this work, C_s = 0.04 mF cm^{-2} was used as the value for the general specific capacitance based on commonly reported values.[46] The CV curves of Pt-NPs-bonded@CNT, Pt−C, and Pt-NPs-attached@CNT under different scan speeds are shown in Figure S11−13. As a result, the C_{dl} becomes an index of the electrochemically active area of the material, as shown in Figure 7a. The C_{dl} is obtained by fitting ΔJ (half of the oxidation and reduction current density) values with different scan speeds of 10, 20, 30, 40, 50, and 60 mV s^{-1}. Consequently, the C_{dl} of the Pt-NPs-bonded@CNT electrode exhibits a significantly higher ECSA value of 7.9 mF cm^{-2} than Pt-NPs-attached@CNT of 5.2 mF cm^2, and the ECSA of Pt−C is 14.8 mF cm^{-2}. Carefully calculated, the electrochemically

https://doi.org/10.1021/acsomega.4c01662
ACS Omega 2024, 9, 21378−21387

active surface area of Pt-NPs-bonded@CNT is 197.5 cm^2, which is significantly larger than the 130 cm^2 of Pt-NPs-attached@CNT, and the electrochemically active surface area of Pt−C is 370 cm^2. The normalization of THE polarization curves by ECSA further indicates that Pt-NPs-bonded@CNT possesses high intrinsic catalytic activity toward the HER and the OER compared with Pt-NPs-attached@CNT and Pt−C, as revealed in Figure 7b−d. This result further demonstrated that platinum nanoparticles anchored on carbon nanotubes with Pt−C bonds possess excellent instinct electrocatalytic activity for hydrogen evolution in acid and alkaline conditions, as well as oxygen evolution ability in alkaline solutions.

4. CONCLUSIONS

Platinum nanoparticles bonded in carbon nanotubes (Pt-NPs-bonded@CNT) with strong Pt−C bonds are successfully established toward ultralow overpotential water splitting ability in alkaline solution with an ampere-level current density. The strong Pt−C bond between Pt nanoparticles and highly conductive carbon nanotubes, can reduce the electron transfer energy barrier and accelerate electron transmission. In addition, platinum nanoparticles bonded in carbon nanotubes can provide more stable active sites. As a result, the Pt-NPs-bonded@CNT electrocatalyst displays distinguished ampere-level electrocatalytic all-water splitting ability in alkaline solution. It exhibits excellent hydrogen evolution in acid and alkaline solutions with ultralow overpotentials of 0.19 and 0.23 V at 1000 mA cm^{-2}, respectively. Besides, it shows superior ampere-level oxygen evolution electrocatalysis in alkaline solution with low overpotential of 1.69 V at 1000 mA cm^{-2}. Moreover, it exhibits high stability over 120 h against hydrogen evolution at 1000 mA cm^{-2} in both acidic and alkaline conditions and long-term stability for 110 h against oxygen evolution in an alkaline solution. It also provides a new strategy for synthesizing new efficient catalysts, otherwise structural optimization for industrial catalytic hydrogen and oxygen evolution.

■ ASSOCIATED CONTENT

Supporting Information

The Supporting Information is available free of charge at https://pubs.acs.org/doi/10.1021/acsomega.4c01662.

TEM images of Pt-NPs-embed@CNT, TEM images of Pt-NPs-attached@CNT, XPS pattern, Tafel slope pattern, LSV curves of Pt-NPs-bonded@CNT-600 °C, CV curves of Pt-NPs-embed@CNT, Pt-NPs-attached@CNT, Pt−C, and RuO_2 at different scan rates (PDF)

■ AUTHOR INFORMATION

Corresponding Author

Hiroshi Sakaguchi − *Department of Materials Science and Engineering, Kyoto University, Kyoto 606-8501, Japan;* orcid.org/0000-0003-1942-907X; Email: sakaguchi@iae.kyoto-u.ac.jp

Authors

Hong Tang − *Institute of Advanced Energy, Kyoto University, Kyoto 611-0011, Japan*

Takahiro Kojima − *Institute of Advanced Energy, Kyoto University, Kyoto 611-0011, Japan*

Kenji Kazumi − *Department of Materials Science and Engineering, Kyoto University, Kyoto 606-8501, Japan*

Kazuhiro Fukami − *Department of Materials Science and Engineering, Kyoto University, Kyoto 606-8501, Japan;* orcid.org/0000-0001-9120-5578

Complete contact information is available at: https://pubs.acs.org/10.1021/acsomega.4c01662

Author Contributions

H.T. conceived the experiments, designing the experiments, carried out the majority of the research and data result analysis, wrote and review the manuscript. T.K. discussed the results and review the manuscript. K.K. performed the material characterized by combining TEM/HRTEM. K.F. performed the material characterized by XRD, XPS, and SEM. H.S. conceived, designed, and supervised the experiments, also review the manuscript. All the authors discussed the manuscript.

Notes

The authors declare no competing financial interest.

■ ACKNOWLEDGMENTS

This study was supported by KAKENHI Program No. 22H01891 (H.S.), 22K18944 (H.S.), 23K04521 (T.K.), Japan Society for the Promotion of Science, Japan; Zero-Emission Energy Research (ZE2022B-07), IAE, Kyoto University (K.F.); Hong Tang, thanks the China Scholarship Council (CSC) for the financial support.

■ REFERENCES

(1) Li, Y.; Xu, T.; Huang, Q.; Zhu, L.; Yan, Y.; Peng, P.; Li, F. F. C_{60} Fullerenol to Stabilize and Activate Ru Nanoparticles for Highly Efficient Hydrogen Evolution Reaction in Alkaline Media. *ACS Catal.* **2023**, *13*, 7597−7605.

(2) Kim, M. G.; Lee, T. K.; Lee, E.; Park, S.; Lee, H. J.; Jin, H.; Lee, D. W.; Jeong, M. G.; Jung, H. G.; Im, K.; et al. Realizing the potential of hydrophobic crystalline carbon as a support for oxygen evolution electrocatalysts. *Energy Environ. Sci.* **2023**, *16*, 5019−5028.

(3) Haase, F. T.; Bergmann, A.; Jones, T. E.; Timoshenko, J.; Herzog, A.; Jeon, H. S.; Rettenmaier, C.; Cuenya, B. R. Size effects and active state formation of cobalt oxide nanoparticles during the oxygen evolution reaction. *Nat. Energy* **2022**, *7*, 765−773.

(4) Wu, Z. Y.; Chen, F. Y.; Li, B.; Yu, S. W.; Finfrock, Y. Z.; Meira, D. M.; Yan, Q. Q.; Zhu, P.; Chen, M. X.; Song, T. W.; et al. Non-iridium-based electrocatalyst for durable acidic oxygen evolution reaction in proton exchange membrane water electrolysis. *Nat. Mater.* **2023**, *22*, 100−108.

(5) Liang, Q.; Li, Q.; Xie, L.; Zeng, H.; Zhou, S.; Huang, Y.; Yan, M.; Zhang, X.; Liu, T.; Zeng, J.; et al. Superassembly of Surface-Enriched Ru Nanoclusters from Trapping-Bonding Strategy for Efficient Hydrogen Evolution. *ACS Nano* **2022**, *16*, 7993−8004.

(6) Chen, X.; Wan, J.; Wang, J.; Zhang, Q.; Gu, L.; Zheng, L.; Wang, N.; Yu, R. Atomically Dispersed Ruthenium on Nickel Hydroxide Ultrathin Nanoribbons for Highly Efficient Hydrogen Evolution Reaction in Alkaline Media. *Adv. Mater.* **2021**, *33*, 2104764.

(7) Ngo, Q. P.; Nguyen, T. T.; Le, Q. T. T.; Lee, J. H.; Kim, N. H. Unveiling the Synergistic Effect of Atomic Iridium Modulated Zirconium-Doped Pure Phase Cobalt Phosphide for Robust Anion-Exchange Membrane Water Electrolyzer. *Adv. Energy Mater.* **2023**, *13*, 2301841.

(8) Wang, H.; Yang, T.; Wang, J.; Zhou, Z.; Pei, Z.; Zhao, S. Coordination Engineering in Single-Site Catalysts: General Principles, Characterizations, and Recent Advances. *Chem* **2024**, *10*, 48−85.

(9) Wan, C.; Zhang, Z.; Dong, J.; Xu, M.; Pu, H.; Baumann, D.; Lin, Z.; Wang, S.; Huang, J.; Shah, A. H.; et al. Amorphous nickel hydroxide shell tailors local chemical environment on platinum

surface for alkaline hydrogen evolution reaction. *Nat. Mater.* **2023**, *22*, 1022−1029.
(10) Zhang, S.; Yin, L.; Wang, S.; Liu, J. C.; Zhang, Y.; Wen, Y.; Zhang, Q.; Du, Y. Ternary Rare Earth Alloy $Pt_{3-x}Ir_xSc$ Nanoparticles Modulate Negatively Charged Pt via Charge Transfer To Facilitate pH-Universal Hydrogen Evolution. *ACS Nano* **2023**, *17*, 23103−23114.
(11) Liu, K.; Yang, H.; Jiang, Y.; Liu, Z.; Zhang, S.; Zhang, Z.; Qiao, Z.; Lu, Y.; Cheng, T.; Terasaki, O.; et al. Coherent hexagonal platinum skin on nickel nanocrystals for enhanced hydrogen evolution activity. *Nat. Commun.* **2023**, *14* (1), 2424.
(12) Chen, J.; Aliasgar, M.; Zamudio, F. B.; Zhang, T.; Zhao, Y.; Lian, X.; Wen, L.; Yang, H.; Sun, W.; Kozlov, S. M.; et al. Diversity of platinum-sites at platinum/fullerene interface accelerates alkaline hydrogen evolution. *Nat. Commun.* **2023**, *14* (1), 1711.
(13) Tan, H.; Tang, B.; Lu, Y.; Ji, Q.; Lv, L.; Duan, H.; Li, N.; Wang, Y.; Feng, S.; Li, Z.; et al. Engineering a local acid-like environment in alkaline medium for efficient hydrogen evolution reaction. *Nat. Commun.* **2022**, *13* (1), 2024.
(14) Liu, S.; Shen, Y.; Zhang, Y.; Cui, B.; Xi, S.; Zhang, J.; Xu, L.; Zhu, S.; Chen, Y.; Deng, Y.; et al. Extreme Environmental Thermal Shock Induced Dislocation-Rich Pt Nanoparticles Boosting Hydrogen Evolution Reaction. *Adv. Mater.* **2022**, *34* (2), 2106973.
(15) Wu, X.; Wang, Z.; Zhang, D.; Qin, Y.; Wang, M.; Han, Y.; Zhan, T.; Yang, B.; Li, S.; Lai, J.; et al. Solvent-free microwave synthesis of ultra-small Ru-Mo_2C@CNT with strong metal-support interaction for industrial hydrogen evolution. *Nat. Commun.* **2021**, *12* (1), 4018.
(16) Zhang, J.; Zhang, L.; Liu, J.; Zhong, C.; Tu, Y.; Li, P.; Du, L.; Chen, S.; Cui, Z. OH spectator at IrMo intermetallic narrowing activity gap between alkaline and acidic hydrogen evolution reaction. *Nat. Commun.* **2022**, *13* (1), 5497.
(17) Yang, Y.; Qian, Y.; Luo, Z.; Li, H.; Chen, L.; Cao, X.; Wei, S.; Zhou, B.; Zhang, Z.; Chen, S.; et al. Water induced ultrathin Mo_2C nanosheets with high-density grain boundaries for enhanced hydrogen evolution. *Nat. Commun.* **2022**, *13* (1), 7225.
(18) Hu, F.; Yu, D.; Zeng, W. J.; Lin, Z. Y.; Han, S.; Sun, Y.; Wang, H.; Ren, J.; Hung, S. F.; Li, L.; et al. Active Site Tailoring of Metal-Organic Frameworks for Highly Efficient Oxygen Evolution. *Adv. Energy Mater.* **2023**, *13* (29), 2301224.
(19) Kim, G.; Jung, S. M.; Giri, A.; Kim, J. S.; Kim, Y. W.; Kim, K. S.; Kim, D.; Choi, Y.; Lee, B. J.; Kim, Y. T.; et al. Enhanced hydrogen desorption via charge transfer in Pt Nanoclusters/ReS_2 hybrid electrocatalyst for efficient hydrogen evolution reaction. *J. Power Sources* **2023**, *579*, 233287.
(20) Wang, Z.; Chen, S.; Wu, W.; Chen, R.; Zhu, Y.; Jiang, H.; Yu, L.; Cheng, N. Tailored Lattice Compressive Strain of Pt-Skins by the $L1_2$ -Pt_3 M Intermetallic Core for Highly Efficient Oxygen Reduction. *Adv. Mater.* **2023**, *35* (36), 2301310.
(21) Zhao, W.; Cui, C.; Xu, Y.; Liu, Q.; Zhang, Y.; Zhang, Z.; Lu, S.; Rong, Z.; Li, X.; Fang, Y.; et al. Triggering Pt Active Sites in Basal Plane of Van der Waals $PtTe_2$ Materials by Amorphization Engineering for Hydrogen Evolution. *Adv. Mater.* **2023**, *35* (29), 2301593.
(22) Pan, Y.; Gao, J.; Lv, E.; Li, T.; Xu, H.; Sun, L.; Nairan, A.; Zhang, Q. Integration of Alloy Segregation and Surface Co?O Hybridization in Carbon-Encapsulated CoNiPt Alloy Catalyst for Superior Alkaline Hydrogen Evolution. *Adv. Funct. Mater.* **2023**, *33* (41), 2303833.
(23) He, F.; Zheng, Q.; Yang, X.; Wang, L.; Zhao, Z.; Xu, Y.; Hu, L.; Kuang, Y.; Yang, B.; Li, Z.; et al. Spin-State Modulation on Metal−Organic Frameworks for Electrocatalytic Oxygen Evolution. *Adv. Mater.* **2023**, *35* (41), 2304022.
(24) Zhang, R.; Li, Y.; Zhou, X.; Yu, A.; Huang, Q.; Xu, T.; Zhu, L.; Peng, P.; Song, S.; Echegoyen, L.; et al. Single-atomic platinum on fullerene C_{60} surfaces for accelerated alkaline hydrogen evolution. *Nat. Commun.* **2023**, *14* (1), 2460.
(25) Park, C. E.; Jeong, G. H.; Theerthagiri, J.; Lee, H.; Choi, M. Y. Moving beyond $Ti_2C_3T_x$ MXene to Pt-Decorated TiO_2@TiC Core-Shell via Pulsed Laser in Reshaping Modification for Accelerating Hydrogen Evolution Kinetics. *ACS Nano* **2023**, *17*, 7539−7549.
(26) Zheng, X.; Shi, X.; Ning, H.; Yang, R.; Lu, B.; Luo, Q.; Mao, S.; Xi, L.; Wang, Y. Tailoring a local acid-like microenvironment for efficient neutral hydrogen evolution. *Nat. Commun.* **2023**, *14* (1), 4209.
(27) Wu, Z.; Liu, X.; Li, H.; Sun, Z.; Cao, M.; Li, Z.; Fang, C.; Zhou, J.; Cao, C.; Dong, J.; et al. A Semiconductor-Electrocatalyst Nano Interface Constructed for Successive Photoelectrochemical Water Oxidation. *Nat. Commun.* **2023**, *14* (1), 2574.
(28) Chen, Y.; Lee, Y.; Chu, W.; Li, J. Trace Ru-tuned NiO/CNT electrocatalysts outperform benchmark Pt for alkaline hydrogen evolution with superior mass activity. *Chem. Eng. J.* **2023**, *472*, 144922.
(29) Zhang, D.; Wang, Z.; Wu, X.; Shi, Y.; Nie, N.; Zhao, H.; Miao, H.; Chen, X.; Li, S.; Lai, J.; et al. Noble Metal (Pt, Rh, Pd, Ir) Doped Ru/CNT Ultra-Small Alloy for Acidic Hydrogen Evolution at High Current Density. *Small* **2022**, *18* (3), 2104559.
(30) Zhang, Y.; Li, G.; Wang, J.; Luo, D.; Sun, Z.; Zhao, Y.; Yu, A.; Wang, X.; Chen, Z. "Sauna" Activation toward Intrinsic Lattice Deficiency in Carbon Nanotube Microspheres for High-Energy and Long-Lasting Lithium−Sulfur Batteries. *Adv. Energy Mater.* **2021**, *11* (26), 2100497.
(31) Yu, W.; Huang, H.; Qin, Y.; Zhang, D.; Zhang, Y.; Liu, K.; Zhang, Y.; Lai, J.; Wang, L. The Synergistic Effect of Pyrrolic-N and Pyridinic-N with Pt Under Strong Metal-Support Interaction to Achieve High-Performance Alkaline Hydrogen Evolution. *Adv. Energy Mater.* **2022**, *12* (21), 2200110.
(32) Jin, H.; Ha, M.; Kim, M. G.; Lee, J. H.; Kim, K. S. Engineering Pt Coordination Environment with Atomically Dispersed Transition Metal Sites Toward Superior Hydrogen Evolution. *Adv. Energy Mater.* **2023**, *13* (11), 2204213.
(33) Zhao, Y.; Kumar, P. V.; Tan, X.; Lu, X.; Zhu, X.; Jiang, J.; Pan, J.; Xi, S.; Yang, H. Y.; Ma, Z.; et al. Modulating Pt-O-Pt atomic clusters with isolated cobalt atoms for enhanced hydrogen evolution catalysis. *Nat. Commun.* **2022**, *13* (1), 2430.
(34) Gu, B. S.; Dutta, S.; Hong, Y. R.; Ngome Okello, O. F.; Im, H.; Ahn, S.; Choi, S. Y.; Woo Han, J.; Ryu, S.; Lee, I. S. Harmonious Heterointerfaces Formed on 2D-Pt Nanodendrites by Facet-Respective Stepwise Metal Deposition for Enhanced Hydrogen Evolution Reaction. *Angew. Chem., Int. Ed.* **2023**, *62* (31), 202307816.
(35) Liu, J.; Li, H.; Wang, J.; Zhang, Y.; Luo, D.; Zhao, Y.; Li, Y.; Yu, A.; Wang, X.; Chen, Z. Design Zwitterionic Amorphous Conjugated Micro-/Mesoporous Polymer Assembled Nanotentacle as Highly Efficient Sulfur Electrocatalyst for Lithium-Sulfur Batteries. *Adv. Energy Mater.* **2021**, *11* (40), 2101926.
(36) Zhang, L.; Liu, L.; Feng, J.; Wang, A. Methanol-Induced Assembly and Pyrolysis Preparation of Three-Dimensional N-Doped Interconnected Open Carbon Cages Supported $FeNb_2O_6$ Nanoparticles for Boosting Oxygen Reduction Reaction and Zn-Air Battery. *J. Colloid Interface Sci.* **2024**, *661*, 102−112.
(37) Li, Y.; Wang, W.; Cheng, M.; Feng, Y.; Han, X.; Qian, Q.; Zhu, Y.; Zhang, G. Arming Ru with Oxygen-Vacancy-Enriched RuO_2 Sub-Nanometer Skin Activates Superior Bifunctionality for pH-Universal Overall Water Splitting. *Adv. Mater.* **2023**, *35* (24), 2206351.
(38) Yan, H.; Jiang, Z.; Deng, B.; Wang, Y.; Jiang, Z. J. Ultrathin Carbon Coating and Defect Engineering Promote RuO_2 as an Efficient Catalyst for Acidic Oxygen Evolution Reaction with Super-High Durability. *Adv. Energy Mater.* **2023**, *13* (23), 2300152.
(39) Da, Y.; Jiang, R.; Tian, Z.; Chen, G.; Xiao, Y.; Zhang, J.; Xi, S.; Deng, Y.; Chen, W.; Han, X.; et al. Development of a Novel Pt_3V Alloy Electrocatalyst for Highly Efficient and Durable Industrial Hydrogen Evolution Reaction in Acid Environment. *Adv. Energy Mater.* **2023**, *13* (16), 2300127.
(40) Wu, S.; Hwang, J.; Matsumoto, K.; Hagiwara, R. The Rational Design of Low-Barrier Fluorinated Aluminum Substrates for Anode-Free Sodium Metal Battery. *Adv. Energy Mater.* **2023**, *13* (48), 2302468.

https://doi.org/10.1021/acsomega.4c01662
ACS Omega 2024, 9, 21378−21387

(41) Liu, J.; Wang, Z.; Wu, X.; Zhang, D.; Zhang, Y.; Xiong, J.; Wu, Z.; Lai, J.; Wang, L. Pt doping and strong metal-support interaction as a strategy for NiMo-based electrocatalysts to boost the hydrogen evolution reaction in alkaline solution. *J. Mater. Chem. A* **2022**, *10*, 15395−15401.
(42) Pei, Z.; Tan, H.; Gu, J.; Lu, L.; Zeng, X.; Zhang, T.; Wang, C.; Ding, L.; Cullen, P. J.; Chen, Z.; et al. A polymeric hydrogel electrocatalyst for direct water oxidation. *Nat. Commun.* **2023**, *14* (1), 818.
(43) Ding, J.; Guo, D.; Wang, N.; Wang, H.; Yang, X.; Shen, K.; Chen, L.; Li, Y. Defect Engineered Metal−Organic Framework with Accelerated Structural Transformation for Efficient Oxygen Evolution Reaction. *Angew. Chem., Int. Ed.* **2023**, *62* (43), No. e202311909.
(44) Wu, D.; Ul Haq, M.; Zhang, L.; Feng, J.; Yang, F.; Wang, A. Noble Metal-Free FeCoNiMnV High Entropy Alloy Anchored on N-Doped Carbon Nanotubes with Prominent Activity and Durability for Oxygen Reduction and Zinc-Air Batteries. *J. Colloid Interface Sci.* **2024**, *662*, 149−159.
(45) Ul Haq, M.; Wu, D. H.; Ajmal, Z.; Ruan, Q. D.; Khan, S.; Zhang, L.; Wang, A. J.; Feng, J. J. Derived-2D $Nb_4C_3T_x$ Sheets with Interfacial Self-Assembled Fe-N-C Single-Atom Catalyst for Electrocatalysis in Water Splitting and Durable Zinc-Air Battery. *Appl. Catal. B-Environ.Energy* **2024**, *344*, 123632.
(46) Zhou, L.; Shao, Y.; Yin, F.; Li, J.; Kang, F.; Lv, R. Stabilizing non-iridium active sites by non-stoichiometric oxide for acidic water oxidation at high current density. *Nat. Commun.* **2023**, *14* (1), 7644.

https://doi.org/10.1021/acsomega.4c01662
ACS Omega 2024, 9, 21378−21387